THE JOURNAL OF COMPARATIVE NEUROLOGY 367:575–594 (1996)

Light Perception in the Vertebrate Brain: An Ultrastructural Analysis of Opsin- and Vasoactive Intestinal Polypeptide-Immunoreactive Neurons in Iguanid Lizards

MICHAEL S. GRACE, VINESSA ALONES, MICHAEL MENAKER, AND RUSSELL G. FOSTER
Department of Biology and National Science Foundation Science and Technology Center for Biological Timing, University of Virginia, Charlottesville, Virginia 22903

ABSTRACT

Recent biochemical and immunocytochemical evidence indicates that a population of circadian and reproductive rhythm-entraining photoreceptors lies in the basal diencephalon of iguanid lizards. Here, we report the results of correlated light and electron microscopy of opsin-immunoreactive cells in the basal brain, and we discuss their ultrastructural relationship to known photoreceptors. Cerebrospinal fluid (CSF)-contacting bipolar neurons in the lizards *Anolis carolinensis* and *Iguana iguana* were immunolabeled with antisera generated against vertebrate retinal opsins and vasoactive intestinal polypeptide (VIP). Within the brain, opsin-immunoreactive cells were found exclusively in the ependyma of the basal region of the lateral ventricles (adjacent to nucleus paraolfactorius/nucleus ventromedialis and neostriatum/paleostriatum). Cells in the same anatomical location and with the same morphology were labeled with anti-VIP antisera. These cells possessed a dendritic process that extended toward the lateral ventricle, ending in a bulbous terminal that protruded into the ventricle. Axonal processes travelled ventrally and caudally. The entire cell, including the axonal process, exhibited opsin-like and VIP-like immunoreactivity. By light microscopy, opsin-like immunostaining appeared punctate, with immunoreactivity greatest in the bulbous terminal. Opsin- and VIP-immunostained thick sections were resectioned, and individual cells observed by light microscopy were then characterized using electron microscopy. We found that all immunostained cells were morphologically similar and that they were morphologically distinct from neighboring nonimmunoreactive cells. CSF-contacting opsin- and VIP-immunoreactive cells lacked the membranous stacks characteristic of retinal photoreceptors but were ciliated and contained numerous large electron-dense vesicles. Multiple synaptic contacts were made on the soma and putative dendritic processes of opsin- and VIP-immunoreactive CSF-contacting neurons. Our results provide the first ultrastructural characterization of opsin-immunostained encephalic CSF-contacting neurons in a vertebrate animal, and they indicate that these putative photoreceptors share structural features with pineal photoreceptors and with certain invertebrate extraretinal photoreceptors, but they are morphologically and biochemically distinct from visual photoreceptors of the retina.

Indexing terms: photoreceptor, immunocytochemistry, cerebrospinal fluid-contacting neuron, retina, pineal

Vertebrate animals utilize two functionally distinct classes of photoreceptors: visual photoreceptors, which mediate image formation, and irradiance detectors, which mediate circadian and other autonomic responses to light. In mammals, photoreceptors responsible for the formation of images and those mediating light regulation of temporal changes in physiology are both located within the eye (Halberg et al., 1954; Dixit et al., 1977; Herbert et al., 1978; Nelson and Zucker, 1981). In nonmammalian vertebrates,

Accepted November 19, 1995.

Address reprint requests to Michael S. Grace, Department of Biology, Gilmer Hall, University of Virginia, Charlottesville, VA 22903. E-mail: msg5y@virginia.edu

these different photosensory roles are spatially segregated. Visual photoreception is mediated by rods and cones of the retina, whereas irradiance detection occurs in the pineal complex (pineal, parapineal, parietal, frontal organ), in the basal brain, and perhaps in the retina as well (Underwood and Menaker, 1970; McMillan et al., 1975a,b).

Numerous studies using a variety of techniques indicate that pineals of many birds, fish, reptiles, and amphibians are photoreceptive. For example, studies on isolated lizard (*Anolis carolinensis*) pineals in vitro (Menaker and Wisner, 1983) and dissociated chicken (*Gallus domesticus*) pineal cells in culture (Takahashi et al., 1989) show that pineals and pinealocytes are directly photoreceptive. Photoreceptors mediating circadian and photoperiodic responses also exist outside the eyes and pineal complex. Combined removal of lateral eyes, pineal organ, and parietal eye fails to abolish circadian entrainment and phase shifting by light in *Sceloporus olivaceous* (Underwood and Menaker, 1970) and in other iguanid lizards (Underwood and Menaker, 1976). In birds, both circadian entrainment and photoperiodic regulation of reproductive state is controlled by photoreceptors outside the eyes and pineal (Benoit, 1935; Menaker and Keatts, 1968; Menaker et al., 1970).

The locations of extraretinal extrapineal photoreceptors have been sought for almost a century. Initial attempts used lesions and/or discreet intracerebral illumination. The results of these experiments indicated that, in birds, photoreceptors mediating photoperiodic responses are located in two regions of the basal brain: the infundibular region of the hypothalamus (Benoit and Ott, 1944; Homma and Sakakibara, 1971; Oliver and Bayle, 1976; Homma et al., 1977; Oliver et al., 1977a,b, 1979; Yokoyama et al., 1978) and the region of the septal and paraolfactory nuclei around the basal lateral ventricles (Homma and Sakakibara, 1971; Oliver et al., 1977, 1980; Sicard et al., 1983).

Vigh and Vigh-Teichmann (Vigh-Teichmann et al., 1980, 1983; Vigh et al., 1983) have argued, based on developmental and ultrastructural similarities between cerebrospinal fluid (CSF)-contacting neurons, pinealocytes, and retinal photoreceptors, that CSF-contacting neurons are likely candidates for basal brain photoreceptors. However, immunocytochemical studies at both the light microscopic and the electron microscopic levels have failed to demonstrate opsin-like immunoreactivity in CSF-contacting neurons of newt (Vigh-Teichmann et al., 1980), frog, and fish (Vigh et al., 1983) hypothalamus.

Several recent studies have provided evidence that a spatially restricted subset of CSF-contacting neurons in the basal brain are photoreceptive. Silver et al. (1988) found opsin-immunoreactive (-IR) CSF-contacting neurons along the lateral ventricle and in the hypothalamus of the quail (*Coturnix coturnix*), duck (*Anas platyrhynchos*), and dove (*Streptopelia risoria*). However, Western blots of brain extracts exhibited multiple immunoreactive bands not corresponding to those in retina, thus failing to confirm the specificity of their antibodies (Silver et al., 1988). Even so, their results are highly suggestive in that immunoreactivity was observed only in areas of the brain thought to contain photoreceptors (see above). Foster et al. (1993) found opsin-IR CSF-contacting neurons in a similar area (lateral ventricular ependyma in the paraolfactory area) of *Anolis carolinenis* brain. In that study, opsin-like immunoreactivity on Western blots appeared as a single band that corresponded in molecular size to retinal opsins. In addition, extracts of *Anolis* anterior brain contained both 11-cis and all-trans retinal (Foster et al., 1993). Subsequently, Garcia-Fernandez and Foster (1993) found opsin-IR cells along the lateral ventricles of lamprey larvae. These cells also showed immunoreactivity with an antiserum against the alpha subunit of the photoreceptor GTP-binding protein (G-protein) transducin. Together with earlier lesion and discreet illumination studies, these results support the idea that opsin-IR CSF-contacting neurons of the lateral ventricles are photoreceptors mediating light-induced changes in temporal physiology in nonmammalian vertebrates.

Here, we report the localization of opsin- and vasoactive intestinal polypeptide (VIP)-IR CSF-contacting neurons in the basal brain of a second iguanid lizard, *Iguana iguana*, and provide an ultrastructural analysis of these cells in both *Iguana* and *Anolis*. We provide evidence that the antigen recognized is immunologically cone opsin-like, and we discuss the possible relationships between opsin-IR CSF-contacting neurons and photoreceptors of the lateral eyes, pineal organ, and parietal eye. These results provide the first ultrastructural analysis of putative encephalic photoreceptors of vertebrates, and they demonstrate that the diencephalic opsin- and VIP-like immunoreactivity observed in this and other recent studies occurs in cells that are similar morphologically to those previously hypothesized to be basal brain photoreceptors.

MATERIALS AND METHODS

Animals

Adult green anoles (*Anolis carolinensis*) were wild caught in Louisiana. Juvenile green iguanas (*Iguana iguana*; approximately 6 months old), bred in captivity, were donated by the Center for Reproduction of Endangered Species, San Diego Zoo (San Diego, CA) or were purchased from Glades Herp, Inc. (Fort Myers, FL). Both groups of animals were maintained at 21°C in constant light, with water available ad libitum. Anoles were fed waxworms, mealworms, and crickets, and iguanas were given a mixture of marmoset chow (Hill's Science Diet, Topeka, KS), kale, collards, and lettuce.

Antisera

The polyclonal anti-chicken cone opsin antisera CERN-874 and CERN-906 were used at dilutions of from 1:500 to 1:4,000. COS-1 is a monoclonal anticone opsin and was used at a dilution of 1:10,000. CERN-JS858, a polyclonal antibovine rhodopsin, was used at 1:1,000. OS-2, a monoclonal antibody recognizing both rod and cone opsins, was used at 1:10,000. CERN-911, which was used at 1:1,000 dilution, recognizes multiple components of the vertebrate phototransduction cascade including transducin (a and b subunits), retinal S-antigen, rhodopsin kinase, and cyclic GMP phosphodiesterase (W.J. DeGrip, personal communication). All of these antibodies were provided by Dr. W.J. DeGrip, University of Nijmegen, The Netherlands. Two different anti-VIP antisera (lot numbers 350201 and 503205; Incstar Corp., Stillwater, MN) were used at dilutions of from 1:1,000 to 1:4,000.

The specificity of binding of antiopsin antisera (except for CERN-911) in an iguanid lizard (*Anolis carolinensis*) has been reported previously (Foster et al., 1993). Two controls were used for nonspecific binding: omission of primary antibody and preadsorption of the serum with purified antigen. Both controls showed no immunoreactivity. Addi-

tion of purified VIP (fragment 10-28; Sigma Chemical Co., St. Louis, MO) to VIP antisera reduced anti-VIP immunostaining in a dose-dependant manner (10–100 μg/ml). Preadsorption of VIP antisera with keyhole limpet hemocyanin-conjugated VIP [coupling agent, 1-ethyl-3-(3-dimethylaminopropyl)carbodiimide] eliminated staining completely.

Light microscopic immunohistochemistry

Lizards were anesthetized by using either cold (*Anolis*) or ketamine (100 mg/kg i.m. at 37°C body temperature; *Iguana*). They were then perfused transcardially with 15 IU/ml heparin in phosphate-buffered saline (PBS; 0.1 M sodium phosphate, 0.9% NaCl, pH 7.4) followed by either Bouin's (75% saturated picric acid, 9.25% formaldehyde, 5% glacial acetic acid) or modified Zamboni's (10% saturated picric acid, 4% paraformaldehyde in 0.1 M sodium phosphate, pH 7.4) fixative. Brains, lateral eyes, pineal glands, and parietal eyes were removed and postfixed overnight in the same fixative with which they were perfused. No differences in morphology or staining pattern were detected between the two fixatives.

For opsin immunohistochemistry, tissues were dehydrated through a graded series of ethanols and xylene and were embedded in paraffin. Serial sections through the entire brain were cut at 20 μm thickness, mounted on gelatin-coated glass slides, deparaffinized in xylene, and rehydrated. Sections were incubated with primary antibody in PBS containing 0.2% Triton X-100 and 1% bovine serum albumin (BSA) for 72 hours at 4°C. For VIP immunohistochemistry, tissues were frozen and cryosectioned either at 10 μm thickness and thaw mounted onto gelatin-coated slides, or at 25 μm thickness and stained free floating. VIP antisera were used in Tris-buffered saline (TBS; 0.02 M Trizma, 0.9% NaCl, pH 7.8) containing 0.25% λ-carrageenan, 1% BSA, and 0.3% Triton X-100 (λ-CBT). Immunolabeling was detected using a Vectastain Elite ABC kit (Vector Laboratories, Burlingame, CA). The color reaction was generated with diaminobenzidine (DAB) and 0.03% hydrogen peroxide. DAB reaction product was intensified in paraffin sections by incubating slides for 2 minutes in a 0.2% aqueous solution of osmium tetroxide. Sections processed for VIP were counterstained with neutral red. Sections were then dehydrated and coverslipped with Permount.

Electron microscopic immunocytochemistry

Animals were anesthetized and perfused with heparin saline followed by a modified Zamboni's fixative [15% saturated picric acid, 4% (w/v) paraformaldehyde, 0.1 or 1.0% glutaraldehyde in 0.1 M sodium phosphate, pH 7.4]. Glutaraldehyde concentration had no significant effect on immunolabeling; staining intensity appeared similar in sections fixed with either 0.1 or 1.0% glutaraldehyde. Brains were postfixed for 1–2 hours in modified Zamboni's fixative without glutaraldehyde and then sectioned by Vibratome at 50 or 60 μm in a bath of ice-cold 0.1 M sodium phosphate. Excess aldehydes were removed by incubating free-floating sections in 1% sodium borohydride in TBS for 30 minutes. Sections were permeabilized by liquid-nitrogen freezing in 10% sucrose, rinsed in TBS, and incubated in primary antiserum diluted in λ-CBT. The antiopsin CERN-874 was used at a dilution of 1:500, and the anti-VIP was used at a dilution of 1:2,000. "No primary" controls were incubated for an equal length of time in λ-CBT alone. Vectastain Elite ABC kit and DAB with glucose-glucose oxidase were used to visualize the reaction. Sections were postfixed flat in 2% osmium tetroxide in 0.1 M phosphate for 20 minutes and were stained en bloc with uranyl acetate. Sections were then dehydrated through alcohols and propylene oxide, infiltrated with propylene oxide/Durcupan resin (Fluka Chemie, Switzerland) mixture, and embedded between Formen Trenmittel (Electron Microscopy Sciences, Fort Washington, PA)-coated glass slides and coverslips in Durcupan resin. Immunopositive sections were photographed, excised from the glass slides, and mounted horizontally onto resin blocks for ultramicrotomy. Thin (silver) sections were mounted onto Formvar-coated copper slot grids and stained with uranyl acetate and lead citrate. Microscopy was performed by using a Jeol 100CX electron microscope.

Densitometric analyses

For densitometric analyses of immunoelectron microscopic material, antiopsin, anti-VIP, and no primary tissues were processed under identical conditions at the same time. All sections were photographed on the same day using identical settings on the electron microscope. Negatives were developed together and were scanned into a Macintosh computer using a flatbed scanner. All images were inverted without further modification. NIH Image was used to perform densitometry on individual vesicles, on regions of cytoplasm devoid of vesicles, mitochondria, or other large subcellular organelles, and on open ventricular space. The average density values of ventricular space varied by less than 5% between electron microscopic images. Density values are on a scale of from 0 (white) to 255 (black).

RESULTS

Light microscopy

Within the brain, the anti-chicken cone opsin antiserum CERN-874 labels only a limited number of pinealocytes and a single distinct group of cells in the basal brains of *Anolis carolinensis* and *Iguana iguana*. These basal brain neurons lie within a thickened region of the ependyma of the basal lateral ventricles (Fig. 1A,B). Examination of serial sections through entire brains of both *Anolis* and *Iguana* indicates that these regions are the only areas of the brain (exclusive of the pineal gland) that are immunoreactive using this opsin antiserum. In both species, only about 500 ependymal cells per brain appear to be immunopositive. There are approximately equal numbers of opsin-IR cells with similar distribution in each hemisphere of the brain (Fig. 1C). Immunoreactive cells are most numerous in the center of the distribution. In *Anolis* basal brain, opsin-IR cells were detected only on the medial aspect of the lateral ventricle (see Fig. 2A), near the rostral portion of the nucleus ventromedialis (NVM) of the septum (Greenburg, 1982). In *Iguana*, these cells are found rostrally on the lateral aspect of the lateral ventricle (adjacent to the paleostriatum and neostriatum) and caudally on the medial aspect of the lateral ventricle [nucleus paraolfactorius (NPO); Distel, 1976; Fig. 1D]. The area of immunostained CSF-contacting neurons occupied approximately 860 μm rostrocaudal, 100 μm dorsoventral on the lateral aspect of the lateral ventricle, and 170 μm on the medial aspect of the lateral ventricle (measured from the bottom of the ependyma) of an *Iguana* brain with the following approximate dimensions: 8.0 mm rostrocaudal (anterior pole to caudal terminus of the third ventricle), 4.7 mm dorsoventral (at the level

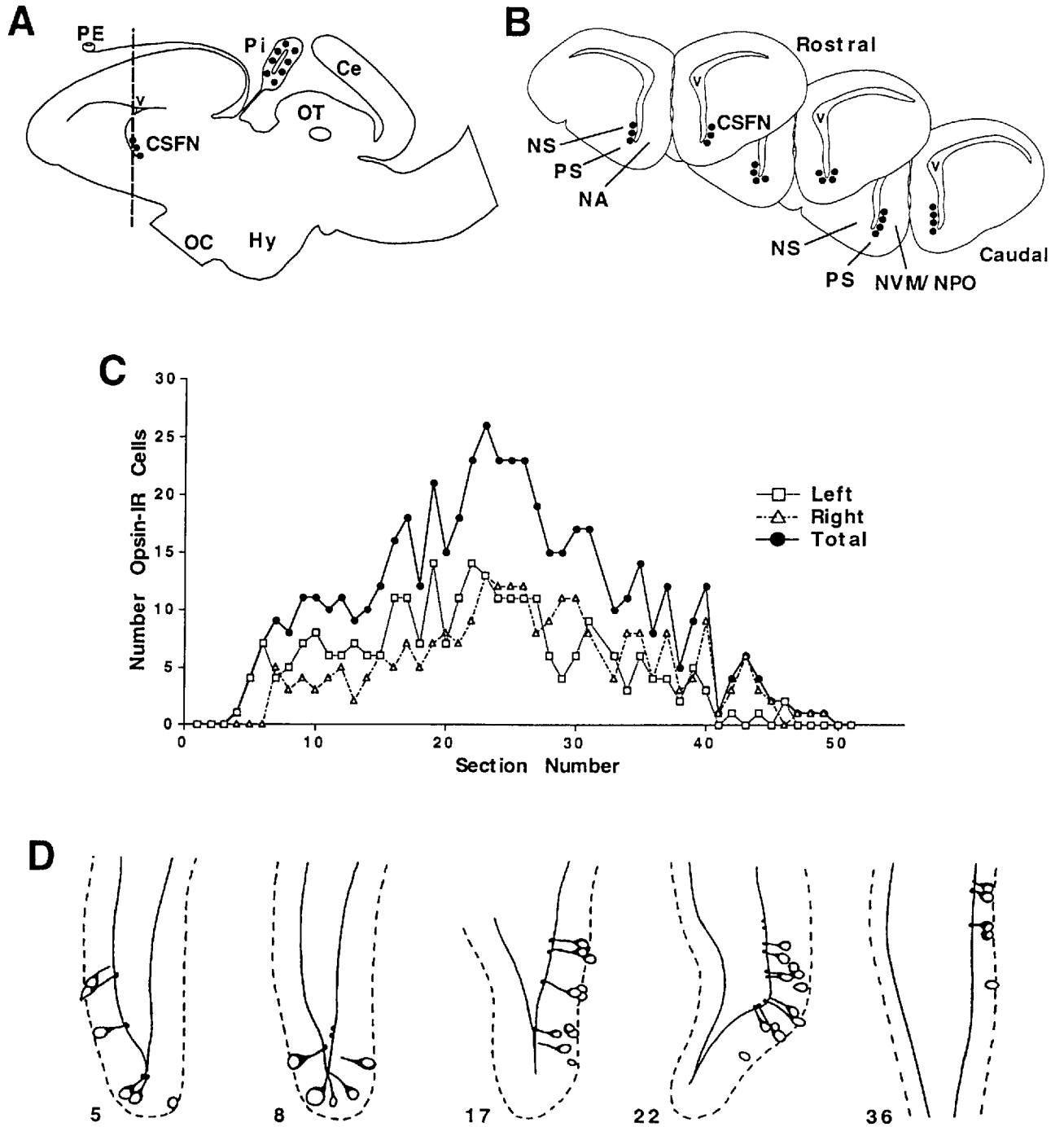

Fig. 1. Location of opsin-like immunoreactivity in *Anolis* and *Iguana* brains. **A:** Sagittal section. **B:** Frontal sections of *Iguana* [frontal sections of *Anolis* contained opsin-immunoreactive (IR) cells only on the medial aspect of the lateral ventricles]. The locations of immunostained cerebrospinal fluid (CSF)-contacting neurons are indicated by solid circles. **C:** Numbers of opsin-IR cells per 20 μm paraffin section of *Iguana* brain. **D:** Camera lucida drawings showing the locations and morphologies of opsin-IR cells in 20 μm paraffin sections of *Iguana* brain. Numbers correspond to section numbers in C. Ce, cerebellum; CSFN, opsin-IR CSF-contacting neurons; Hy, hypothalamus; NA, nucleus accumbens; NPO, nucleus paraolfactorius; NS, neostriatum; NVM, nucleus ventromedialis; OC, optic chiasm; OT, optic tectum; PE, parietal eye; Pi, pineal; PS, paleostriatum; V, ventricle.

of the optic chiasm), and 8.0 mm bilateral (at the level of the pineal).

Immunoreactive cells have an elliptical soma of approximately 5–7 μm diameter and a process that extends toward the ventricle and terminates in an intensely stained bulbous terminal that appears to protrude into the ventricular lumen (Fig. 2B,D–F). This putative dendritic process in *Iguana* is typically longer and thinner than in *Anolis*. Immunoreactive CSF-contacting neurons are labelled throughout the cell. The soma and the presumptive den-

dritic process both exhibit a punctate staining pattern. A varicose immunoreactive process (presumptive axon) extends from the soma in a ventrocaudal direction (Fig. 2C,G). Numerous varicose immunoreactive fibers were observed in the hypothalamic region. Only a subset of ependymal cells are opsin-IR; cells immediately adjacent to opsin-IR CSF-contacting neurons show no apparent immunoreactivity (Fig. 2D–F).

Similarly, only a subset of pinealocytes are immunoreactive in both *Anolis* and *Iguana* (Fig. 2I), whereas all retinal photoreceptors react with CERN-874. Pinealocytes exhibiting opsin-like immunoreactivity appear otherwise to be morphologically identical to unlabeled cells and are apparently distributed randomly throughout the pineal. Most immunopositive pinealocytes exhibit opsin-like immunoreactivity throughout the cell. Outer segments are most intensely labeled, and, in some cases, the outer segment is the only portion of the cell that is labeled. Often, however, outer segments, cell bodies, and axons are all immunostained (Fig. 2I). Opsin-like immunoreactivity was undetectable in the parietal organs of both *Anolis* and *Iguana*.

Other antisera developed to recognize photoreceptor opsins were tested for their ability to label CSF-contacting neurons and pinealocytes. The results indicate that, in iguanid lizards, cone-specific (but not rod-specific) antibodies label these cells. In addition to CERN-874, two other cone-specific antisera, CERN-906 and COS-1, label CSF-contacting neurons of the lateral ventricles (see Foster et al., 1993), whereas the rod-specific CERN-S858 and the rod/cone-specific OS-2 failed to do so. Similar to CERN-874, CSF-contacting neurons of the NVM of the septum and pinealocytes are the only cells in the brain that are labeled by CERN-906 and COS-1. CERN-911 immunolabeled a subset of both retinal and pineal photoreceptors as well as a subset of cells in the inner nuclear layer of the retina but failed to immunolabel CSF-contacting neurons of the lateral ventricular ependyma.

CSF-contacting neurons of the lateral ventricular ependyma of both *Anolis* and *Iguana* were also labelled with antisera to VIP (Fig. 3). These cells are morphologically identical to those immunolabeled with antiopsin antisera. VIP-like immunoreactivity was very intense and occurred throughout the cell, including the axon and the intraventricular dendritic terminal (Fig. 3).

Electron microscopy

Correlated light and electron microscopy was used to unequivocally identify opsin-IR cells in electron micrographs. The anticone opsin antiserum CERN-874 was used for all electron microscopic studies of opsin immunoreactivity. Thick (50 μm) Vibratome sections permeabilized by freezing and by limited exposure to low levels of detergent exhibited immunoreactive cells on both surfaces of the section, but not deep within it. After photographing these immunoreactive cells at the light level, the surfaces of thick sections were resectioned by ultramicrotomy. Individual cells as well as clusters of cells identified as immunoreactive at the light microscopic level were identified by electron microscopy (Figs. 4, 5). Various features, including the presence of an intraventricular bulbous terminal, the shape and size of the soma, the shape of the putative dendritic process, and the location of nuclei and nucleoli, confirmed the identity of cells observed by electron microscopy as the same immunostained cells seen by light microscopy. These cells were very lightly stained. The numerous large vesicles were very electron dense, whereas the cytoplasm was more electron lucent than adjacent, unstained ependymal cells (Figs. 4, 5; see below).

Electron microscopy of VIP-IR CSF-contacting neurons revealed that DAB reaction product was distributed throughout the cytoplasm, including that within the soma and within the dendrite and its terminal (Fig. 6). Otherwise, VIP-IR cells were ultrastructurally identical to those immunostained with CERN-874.

At the light microscopic level, only a subset of ependymal cells in the region of the NVM/NPO express opsin-like or VIP-like immunoreactivity. Electron microscopy reveals that all basal forebrain cells exhibiting immunoreactivity share similar morphological characteristics and that all cells exhibiting these characteristics are opsin- or VIP-IR. Furthermore, opsin-IR CSF-contacting neurons of the basal forebrain are distinct from adjacent nonimmunostained cells in the basal brain in several ways (Figs. 4–7). In addition to the subcellular features described below, opsin-IR CSF-contacting neurons exhibit a relatively electron-lucent cytoplasm and nucleus; the nuclei are spherical, whereas those of adjacent nonimmunoreactive cells are elongated and often lobed (see, e.g., Figs. 4, 7). Nonvillous opsin-IR neurons have been observed only in regions of the ventricular ependyma containing primarily villous epithelial cells. The cell bodies of opsin-IR CSF-contacting neurons are typically located at the edge of the ependyma adjacent to the neuropil.

To determine more precisely the location of opsin- and VIP-like antigens, densitometric analyses were performed on opsin- and VIP-immunostained as well as on "no primary" material. Cells with the same set of characteristics and in the same anatomical location were identified in material that had been processed as for immunocytochemistry, with the exception that the primary antiserum was omitted (no primary; Fig. 7). We identified putative encephalic photoreceptors of the lateral septum in "no primary" material by staining alternate serial sections for opsin or VIP. Opsin-IR cells appear to be much lighter at the ultrastructural level than anticipated, but the immunoreactivity appears to be concentrated in the large electron-dense cytoplasmic vesicles. Densitometry of electron microscopic negatives demonstrates that these vesicles are more electron dense in opsin-immunostained material than in tissue incubated without primary antiserum, whereas cytoplasmic electron density is slightly higher in opsin-immunostained than in "no primary" material (Fig. 8; cytoplasmic values were determined by using the terminal and adjacent dendritic region). VIP-immunostained material exhibits greater electron density than control material in both vesicle and cytoplasmic domains (Fig. 8).

The terminals of opsin- and VIP-IR ependymal neurons lie within the lateral ventricles. In many preparations, the ventricle is artifactually expanded, but the conclusion that the bulbous terminal lies within the ventricle is supported by observations of intraventricular terminals in sections in which the two sides of the ventricle are tightly apposed (Fig. 9). In addition, opsin-IR neurons form junctional complexes (zonulae) with adjacent nonimmunoreactive epithelial cells (Fig. 10), and these complexes occur where the dendrite abruptly expands and forms the bulbous terminal that protrudes through and past the ventricular epithelial microvilli.

Numerous electron-dense vesicles lie within the cytoplasm of opsin- and VIP-immunostained CSF-contacting

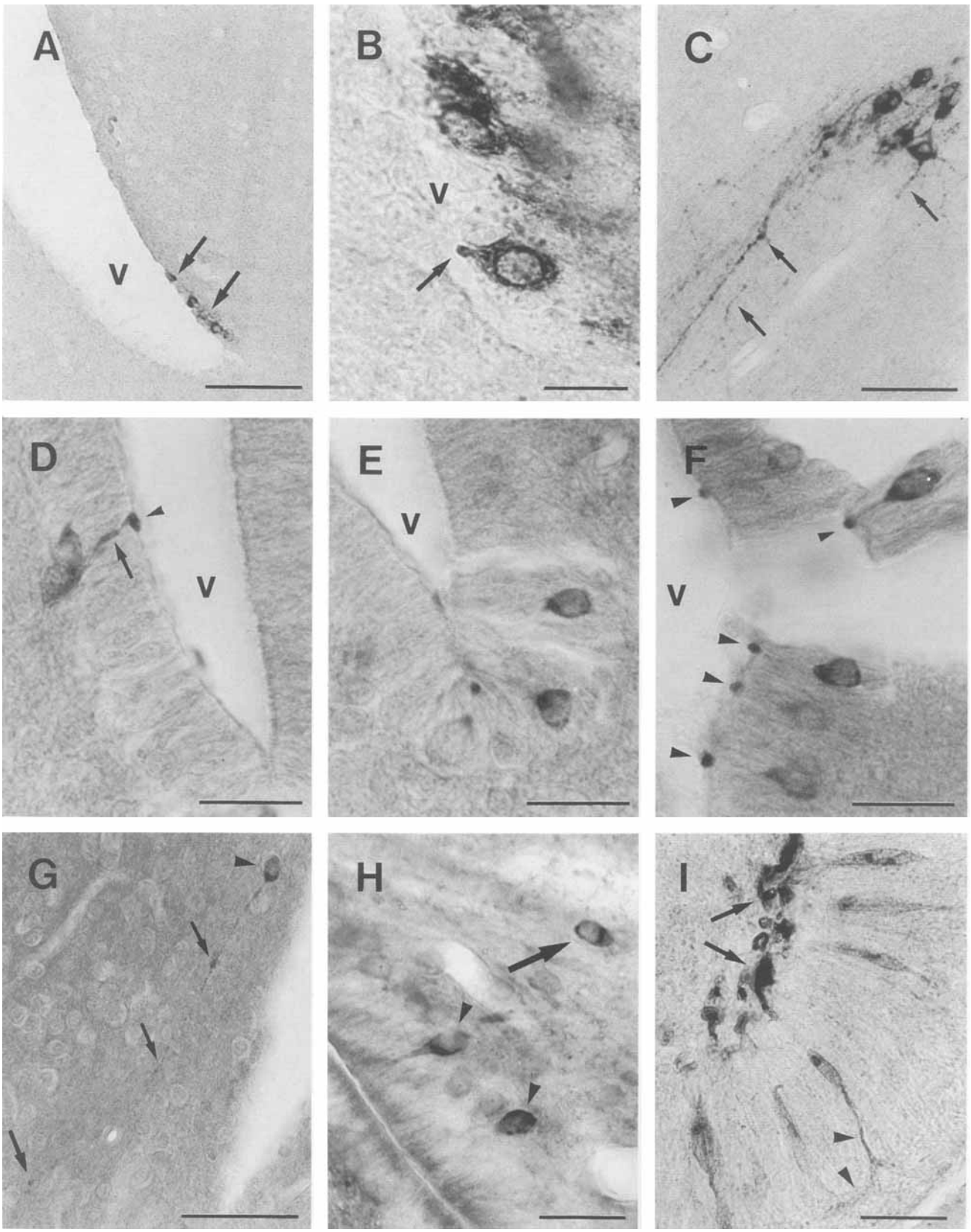

Figure 2

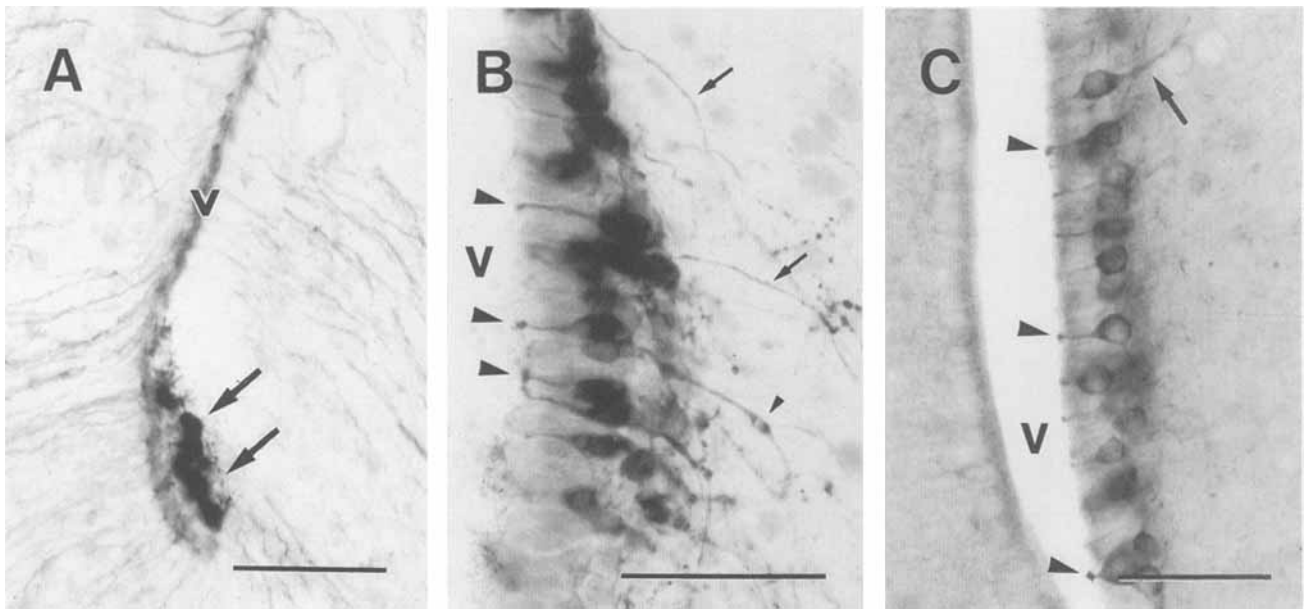

Fig. 3. Light micrographs of vasoactive intestinal polypeptide (VIP)-IR cells in the basal forebrain of *Anolis* and *Iguana*. **A:** Immunostained cells (arrows) on the medial aspect of the lateral ventricle of *Anolis*. **B:** VIP-like immunoreactivity in CSF-contacting neurons of *Iguana*. Note the bulbous terminals (large arrowheads) at the border of the lateral ventricle (v) and the immunostained neurites (arrows). A single bipolar neuron located outside the ependyma is immunostained (small arrowhead). Counterstained with neutral red. **C:** VIP-like immunoreactivity in 50 μm Vibratome section of glutaraldehyde-fixed *Iguana* brain. CSF-contacting terminals (arrowheads) and an axon (arrow) are immunostained. Scale bars = 50 μm.

neurons (Fig. 11). These vesicles are large (typical diameter, 70–120 nm) and occur throughout the soma and the putative dendritic process and within the intraventricular terminal, where they are most highly concentrated (Fig. 11A). There is no apparent association of vesicles with other subcellular structures (Fig. 11B). Vesicles are much more numerous in *Anolis* (compared to *Iguana*) preparations, often nearly filling the cytoplasm in all regions of the cells (Fig. 11C). These vesicles are membrane bound, and they exhibit a granular internal appearance (Fig. 11D). They show varying degrees of electron density; some are extremely dense, and others are relatively electron lucent. Whereas these electron-dense vesicles may contain the opsin-like antigen, the cytoplasm, particularly within the intraventricular terminals, often exhibits the granular electron-dense appearance of oxidized DAB (Fig. 11A; see also Figs. 5, 8), suggesting the presence of cytoplasmic opsin-like immunoreactivity.

Opsin- and VIP-IR CSF-contacting neurons contain axonemes. Basal bodies have been observed both in the soma (*Anolis*; Fig. 12A,B) and in the ventricular terminal (*Iguana*; Fig. 12C). Because tissue was sectioned parallel to the long axis of the cell, we rarely observed axonemes in cross section. However, in *Anolis* material, we observed one distinct cross section of an axoneme (Fig. 12D) lacking the central pair of microtubules (the "9+0" arrangement characteristic of ciliated sensory cells, including retinal photoreceptors). Ciliary rootlets were often observed in sections of *Iguana* CSF-contacting neurons (Fig. 12E,F) coursing long distances through the putative dendritic process.

Multiple synaptic contacts occur on opsin- and VIP-IR neurons (Fig. 13) and have been observed most often on the presumptive dendritic process (Fig.13B), although they also occur on the soma (Fig 13C). The identity of the presynaptic neurons is unknown. Boutons synapsing onto immunoreactive CSF-contacting neurons are morphologically similar in *Anolis* and *Iguana* preparations. They are characterized by numerous spherical electron-lucent vesicles, fewer electron-dense vesicles, and both pre- and postsynaptic membrane densities. On a single immunoreactive CSF-contacting neuron, as many as four synaptic contacts have been observed (Fig. 13B).

Fig. 2. Light micrographs of opsin-IR CSF-contacting neurons in *Anolis carolinensis* and *Iguana iguana*. The antiserum used was CERN-874. **A:** Low-power light micrograph showing the highly localized antiopsin immunostaining (arrows) in *Anolis carolinensis* basal brain (v, lateral ventricle). **B:** Immunostained cells along the medial aspect of the lateral ventricle of *Anolis*. Note the bulbous terminal (arrow) extending into the lumen of the ventricle (v). **C:** Sagittal section of *Anolis* brain showing immunostained processes (arrows) traveling ventrally and caudally. **D:** Immunostained CSF-contacting neurons in the ependyma of the lateral aspect of the lateral ventricle (v) of *Iguana*. Note the stained dendrite (arrow) and terminal (arrowhead). **E:** Immunostained cells at the base of the lateral ventricle (v) in *Iguana*. **F:** Immunostained cells on the medial aspect of the lateral ventricle of *Iguana*. Note the intensely stained terminals (arrowheads) that contact the ventricular lumen (v). **G:** Tangential section of *Iguana* brain showing an immunostained neuron (arrowhead) and its stained varicose axonal process (arrows) running in a ventrocaudal direction. **H:** Vibratome section (50 μm) of *Iguana* brain showing several immunostained ependymal CSF-contacting neurons (arrowheads) and a "displaced" immunostained neuron (arrow). **I:** *Anolis* pineal showing intensely stained pinealocyte outer segments (arrows), soma, and axon (arrowheads). Only a limited number of pinealocytes exhibit immunoreactivity. Scale bars = 50 μm in A,G, 10 μm in B, 20 μm in C–F, 30 μm in H,I.

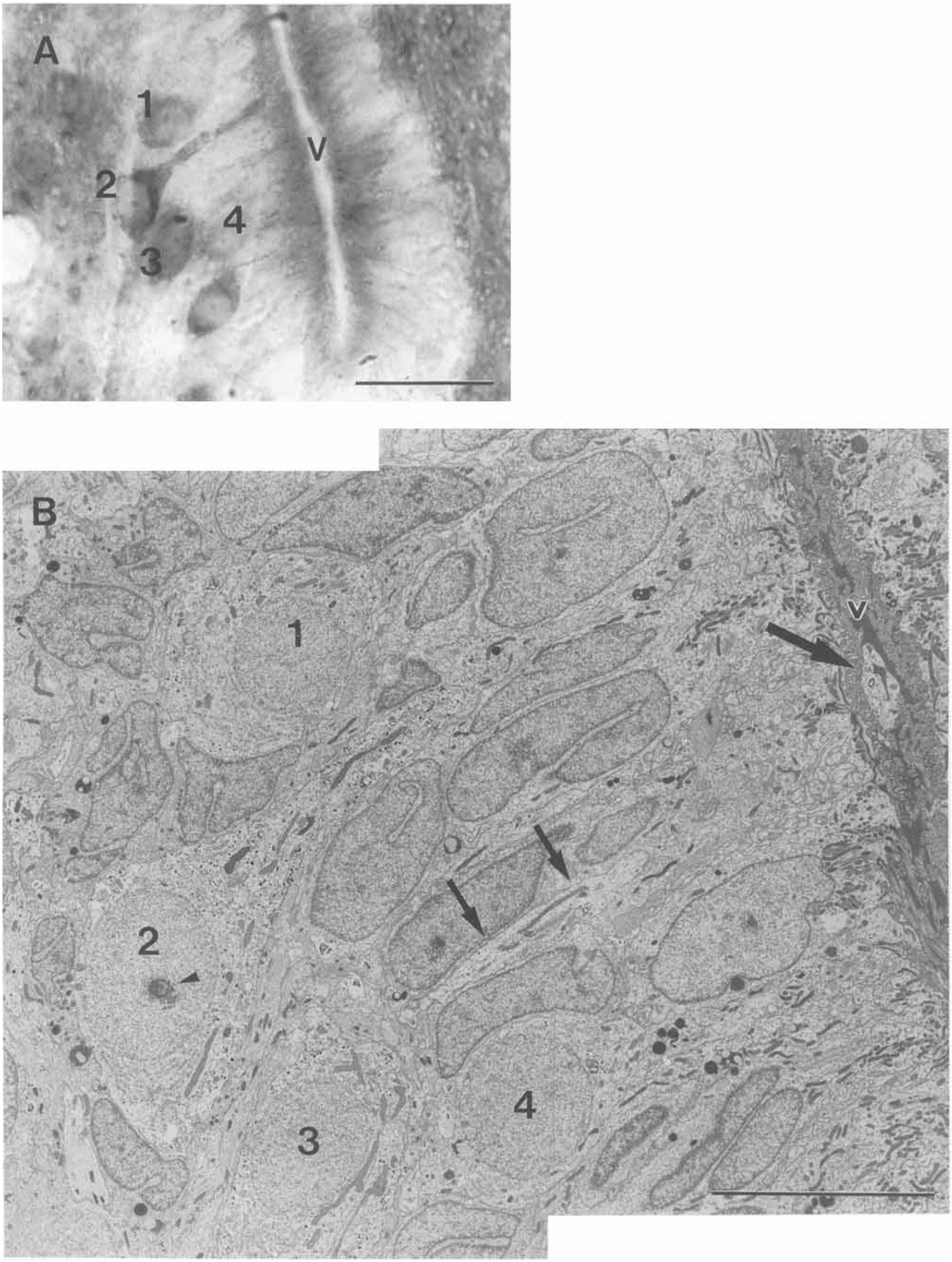

Fig. 4. Corresponding light and electron micrographs of opsin-IR CSF-contacting neurons in *Iguana* basal brain. **A:** Opsin-immunostained (CERN-874) 50-μm-thick section showing a group of immunostained CSF-contacting neurons adjacent to the lateral ventricle (v). **B:** Electron micrograph of a thin section taken from the thick section shown in A. Note that the four cells labeled in A are easily distinguishable. Note in particular the shapes and positions of nuclei, the shape of the soma, and the position of the nucleolus (arrowhead) in cell 2. A portion of the dendrite (small arrows) and the intraventricular terminal (large arrow) of cell 3 can be seen within the ventricle (v). Scale bars = 30 μm in A, 10 μm in B.

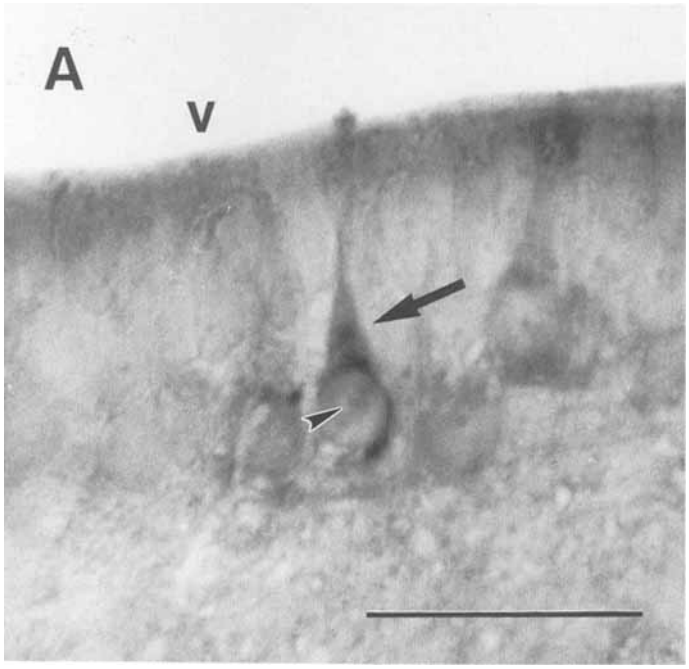

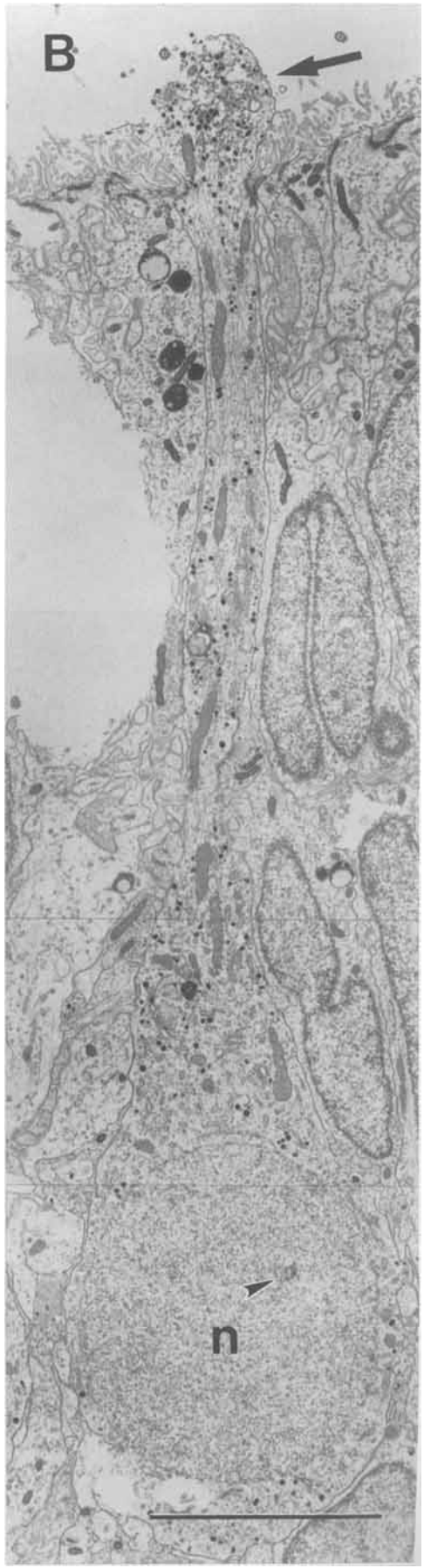

Fig. 5. Light and electron micrographs of a single CSF-contacting neuron in the ependyma of the *Iguana* lateral ventricle. **A:** Light micrograph of an opsin-immunostained cell (arrow; v, ventricle). **B:** Electron micrograph of the cell indicated in A showing the entire profile of the cell from its soma to the intraventricular terminal (arrow; n = nucleus). Note the s-shaped curve of the dendrite and the position of the nucleolus (arrowheads in A and B). Scale bars = 30 μm in A, 5 μm in B.

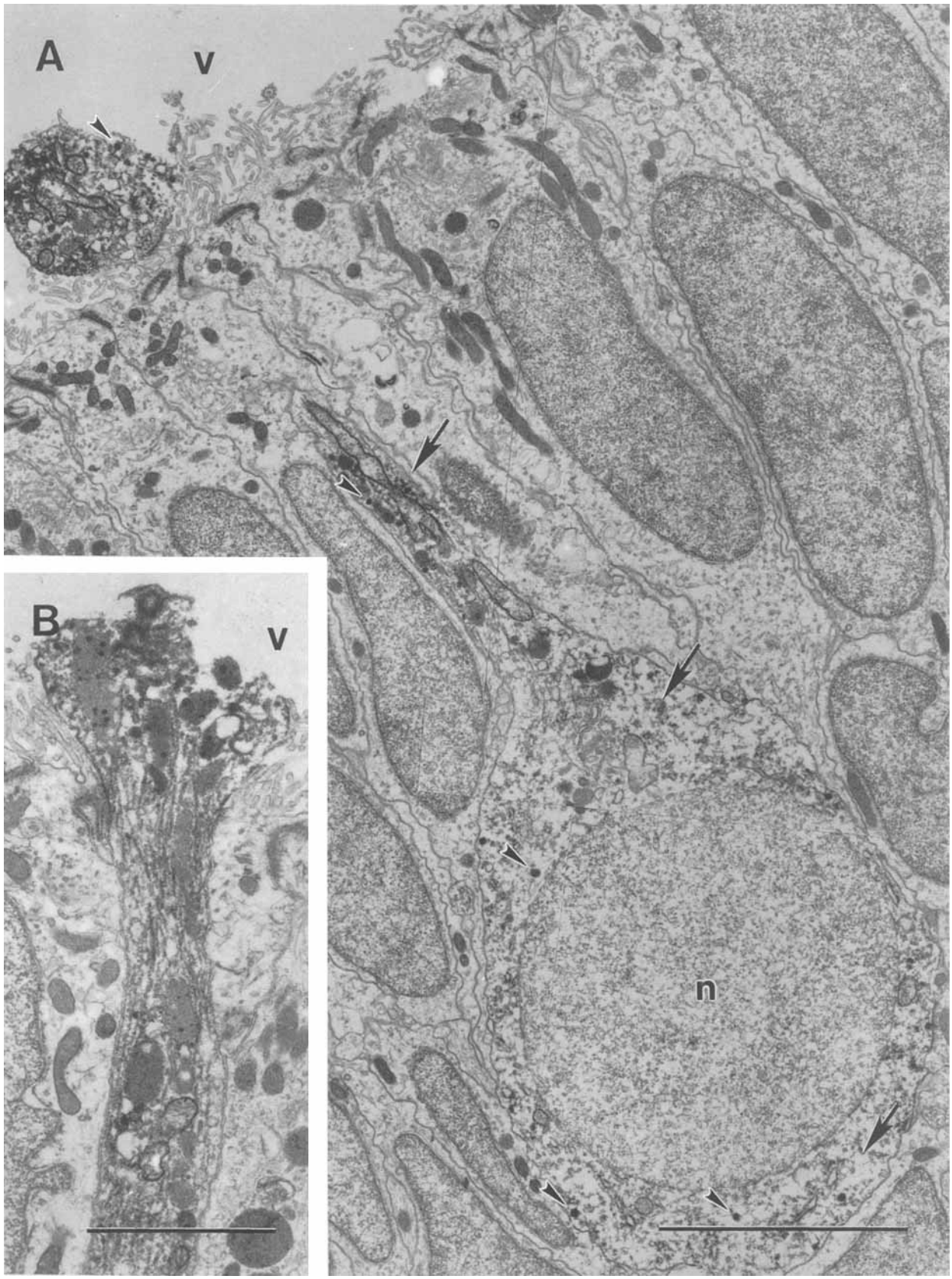

Fig. 6. Electron micrographs of VIP-IR CSF-contacting neurons of *Iguana*. **A:** A single VIP-immunostained CSF-contacting neuron. A portion of the neurite connecting the soma and ventricular terminal (v) is not visible in this section. Note the granular diaminobenzidine reaction product in the cytoplasm (arrows) and the electron-dense vesicles (arrowheads) scattered throughout the cytoplasm. Note also the spherical, relatively electron-lucent nucleus (n). **B:** The terminal of a VIP-immunostained neuron contacting the lumen of the lateral ventricle (v). Scale bars = 5 μm in A, 2 μm in B.

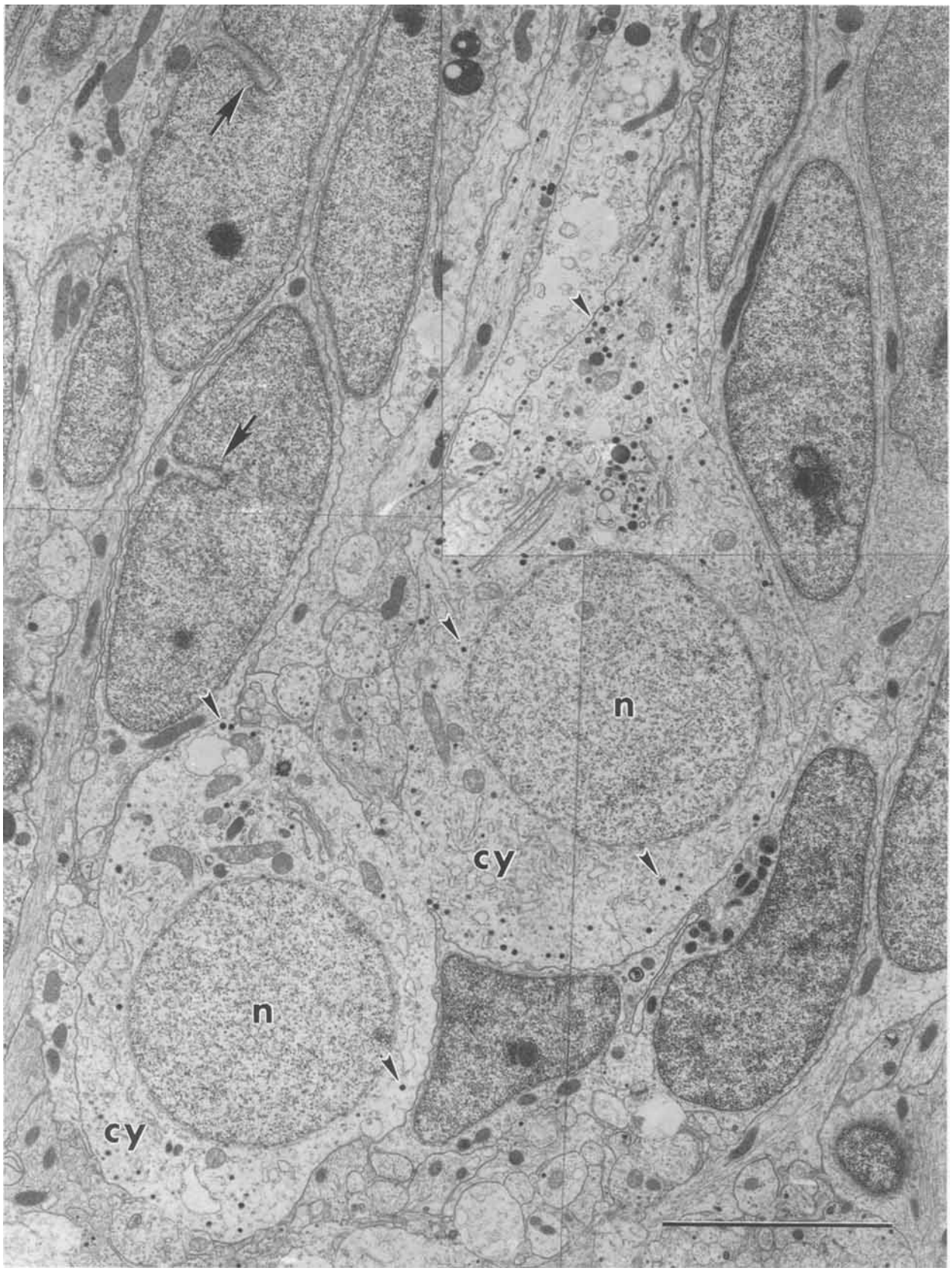

Fig. 7. Electron micrograph of *Iguana* tissue treated as immunostained material, except that primary antiserum was omitted. Two CSF-contacting neurons of the basal lateral ventricular ependyma exhibit characteristic electron-dense vesicles (arrowheads) and electron-lucent cytoplasm (cy) and nuclei (n) relative to adjacent ependymal cells. Note also that nuclei of CSF-contacting neurons are spherical, whereas those of adjacent ependymal cells are elongated and often lobed (arrows). Scale bar = 5 μm.

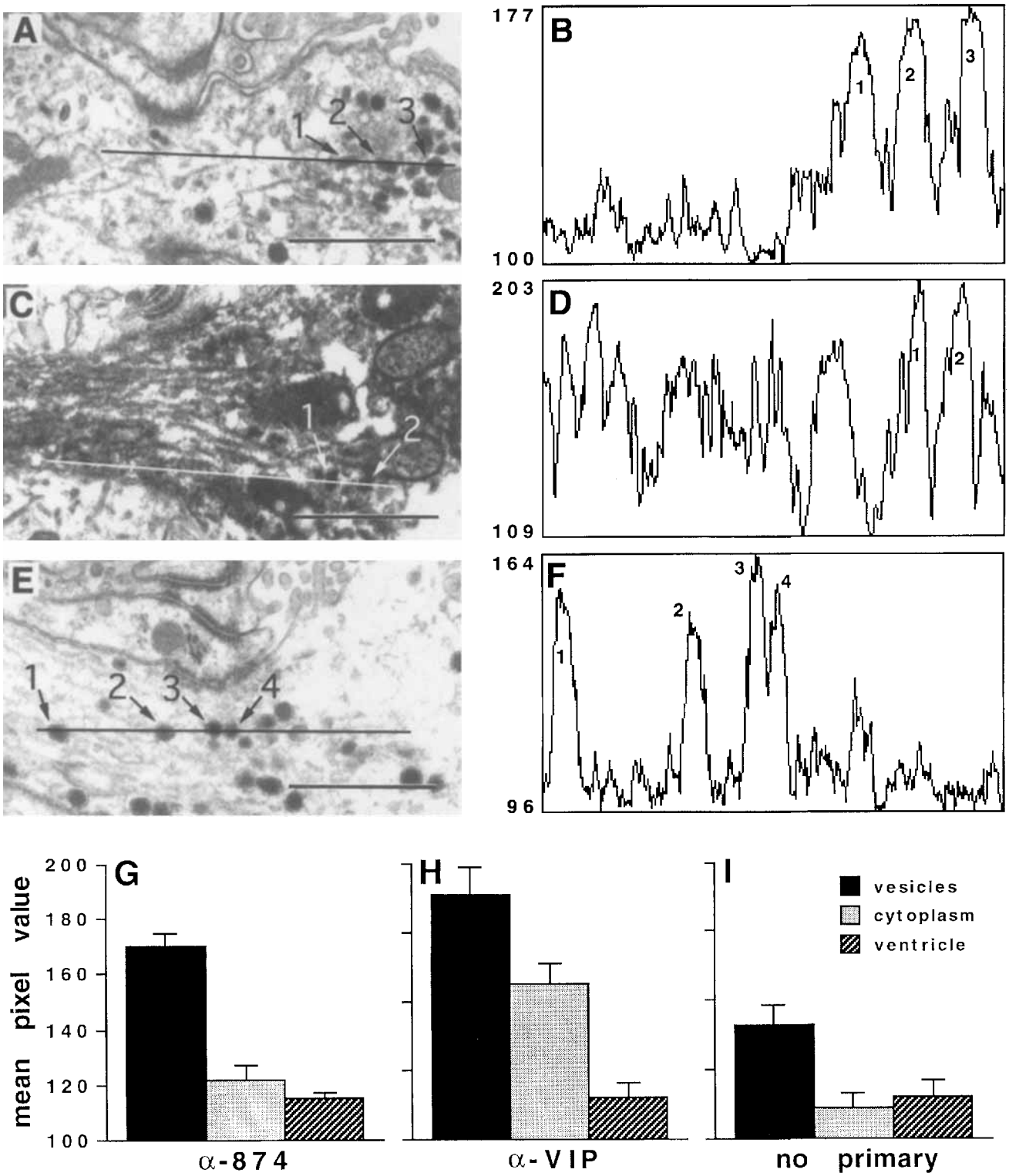

Fig. 8. **A–I:** Densitometry of electron micrographs of immunostained CSF-contacting neurons from *Iguana*. A,C,E: Electron micrographs of opsin-immunostained, VIP-immunostained, and "no primary" control materials, respectively. B,D,F: Plots of density values determined along the lines shown in A, C, and E, respectively. Electron-dense vesicles and their corresponding density peaks are numbered as landmarks. Density values are on a scale of 0–255, with 0 representing white and 255 representing black. G,H,I: Histograms of mean pixel values from opsin-immunostained, VIP-immunostained, and "no primary" control materials, respectively. Average pixel values were determined for vesicles, open ventricular space, and regions of cytoplasm devoid of large subcellular organelles. Numbers of regions sampled (vesicles, cytoplasm, and ventricle, respectively): opsin immunostained, 36, 25, and 19; VIP-immunostained, 20, 29, and 20; "no primary", 30, 22, and 16. Values indicate mean ± standard deviation. Scale bars = 1 μm in A,C,E.

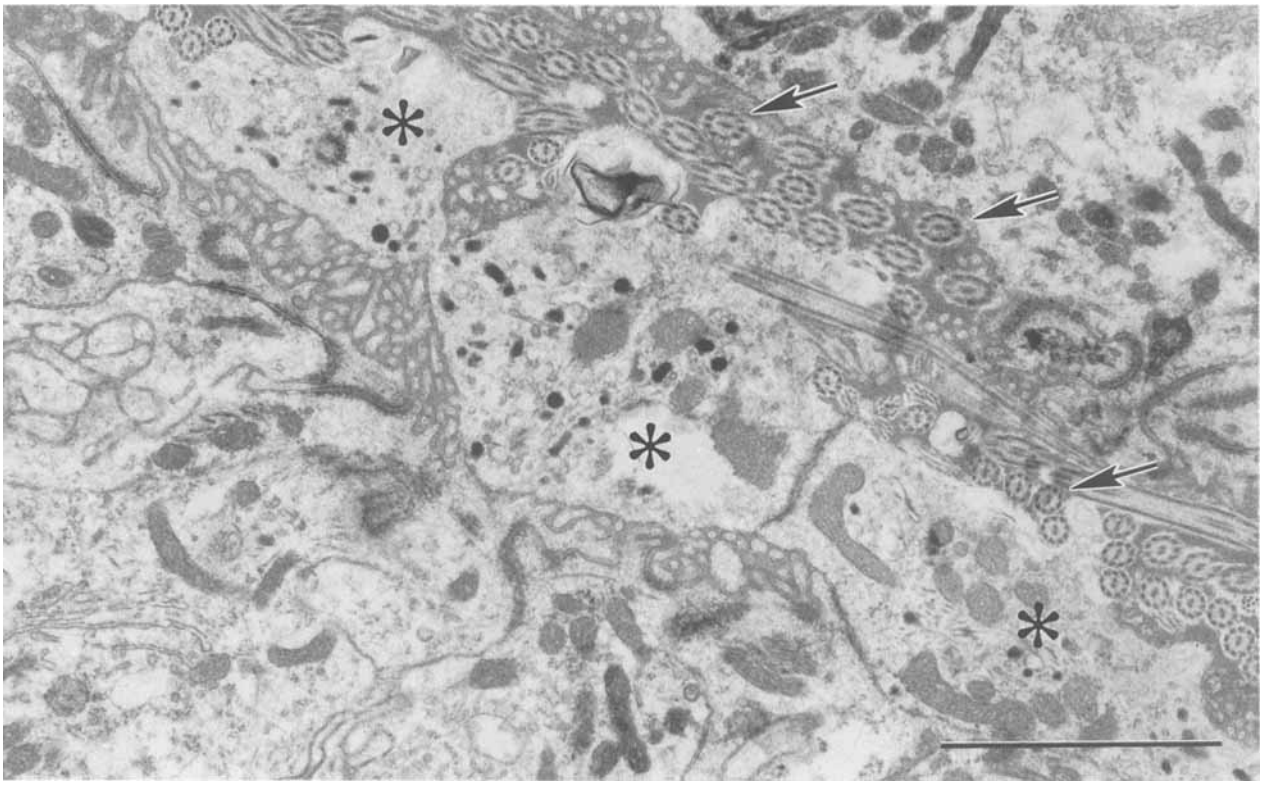

Fig. 9. Electron micrograph showing three terminals (asterisks) of *Iguana* opsin-IR ependymal neurons lying between the tightly apposed walls of the lateral ventricle. The cells from which these terminals arise are located on the microvillus side of the ventricle (lower left). Note the numerous "9+2" cilia that arise from cells on the opposite side of the lateral ventricle. Scale bar = 2 μm.

DISCUSSION

A combined light and electron microscopic immunohistochemical approach was used to visualize opsin-IR CSF-contacting neurons. This unequivocal identification of individual immunoreactive neurons allowed a detailed examination of the ultrastructure of these putative circadian photoreceptors.

Although a direct demonstration of photosensitivity has yet to be shown, several lines of evidence support the hypothesis that CSF-contacting neurons of the lateral ventricle ependyma are photoreceptors. In addition to the results reported here and in another *Anolis* study (Foster et al., 1993), opsin-like immunoreactivity has been found in ventricular ependymal cells with similar morphology in birds (Silver et al., 1988) and in Agnatha (Garcia-Fernandez and Foster, 1993). Opsin-like immunoreactivity has been detected on Western blots of *Anolis carolinensis* anterior brain extracts (Foster et al., 1993). This single immunoreactive band corresponded in molecular size to opsin in *Anolis* retinal homogenates.

Other components of the phototransduction cascade also occur in the vertebrate brain. For example, Garcia-Fernandez and Foster (1993) found transducin-like immunoreactivity in CSF-contacting neurons of the hypothalamic periventricular area of larval lampreys (*Petromyzon marinus*). CSF-contacting neurons of the same region were labeled with antiopsin antisera. Phototransduction-associated retinoids have been identified in the brain. Foster et al. (1993) found both 11-cis- and all-trans-didehydroretinaldehyde (vitamin A2) in the anterior brain of *Anolis carolinensis* (Provencio et al., 1992). Vitamin A2 is the visual chromophore in both retinal and pineal photoreceptors in *Anolis*.

The opsin family of proteins is a subset of seven transmembrane-spanning proteins, including several types of receptors. The polyclonal antiserum used in this study, therefore, might be expected to cross react with other members of this receptor superfamily. However, in serial sections through the entire brains of both *Anolis* and *Iguana*, immunoreactivity was observed only in CSF-contacting neurons of the basal lateral ventricles and in a subset of pinealocytes. In retina, the antiserum labeled only photoreceptor inner and outer segments. These results suggest that immunoreactivity in CSF-contacting neurons indicates the presence of an opsin-like protein.

It is unclear whether the putative opsin present in CSF-contacting neurons is cone- or rod-like. In iguanid lizards, antisera specific for cone opsins stain CSF-contacting neurons, whereas both an antiserum labelling cones and rods and a rod-specific antiserum failed to label these cells. These results suggest that the antigen recognized may be cone opsin-like. However, the monoclonal antibody RET-P1, which is specific for rod photoreceptors in the retina, labeled CSF-contacting neurons in several birds (Silver et al., 1988). In fact, opsin-like immunoreactivity has been detected in the septum and/or hypothalamus of representatives of all four nonmammalian vertebrate classes and in Agnatha (for review, see Foster et al., 1994).

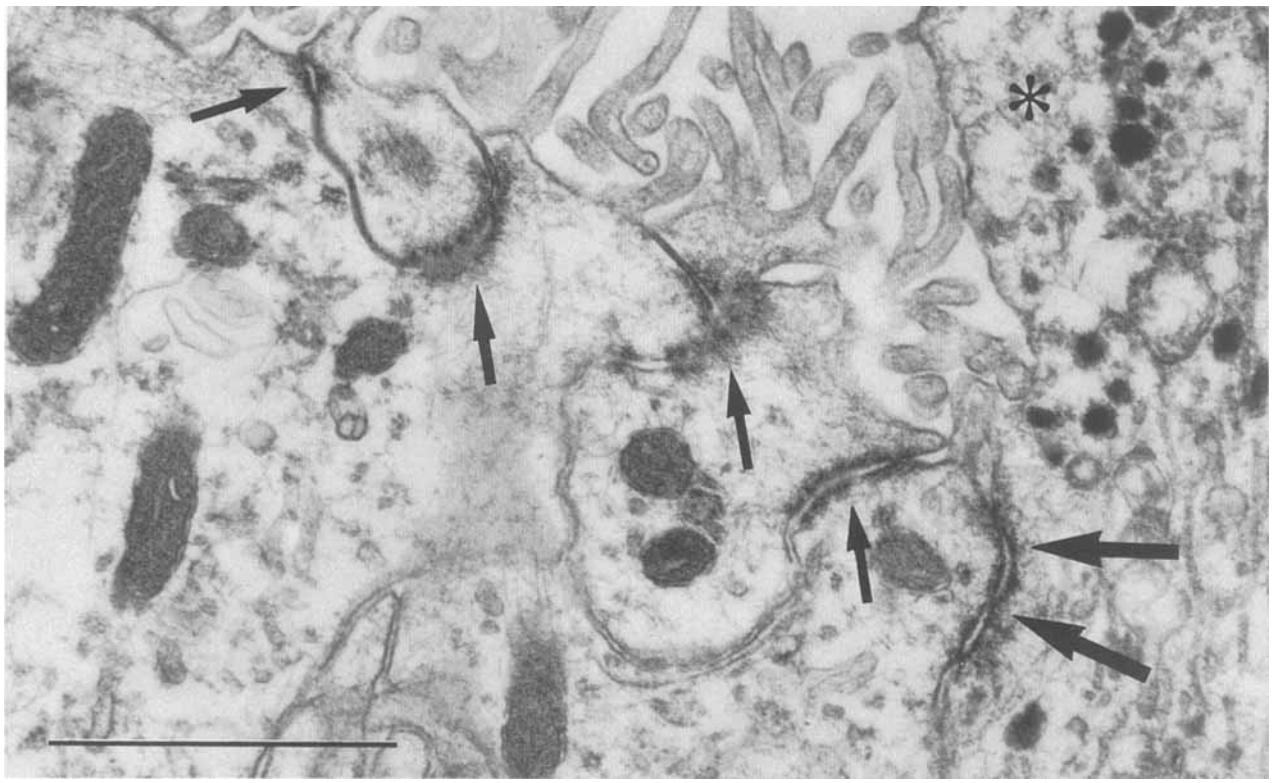

Fig. 10. Electron micrograph showing that opsin-IR CSF-contacting neurons in *Iguana* form junctions with adjacent nonimmunoreactive ependymal cells. These junctions (large arrows) occur between the dendritic process and the apical aspects of adjacent microvillus epithelial cells and only at the base of the intraventricular terminal (asterisk). Small arrows indicate junctions between neighboring nonimmunoreactive epithelial cells. Scale bar = 1 μm.

In some species, immunoreactivity was rod-like (e.g., goldfish; Foster et al., 1994); in others, it was cone like (e.g., *Anolis carolinensis*: Foster et al., 1993; Grace et al., 1993; other anoline lizards and *Gekko gekko*: Foster et al., 1994); and, in Agnatha, it was rod and cone like (Garcia-Fernandez and Foster, 1993). There may be multiple types of opsin within encephalic photoreceptors, or the photopigment may share features with both rod and cone opsins.

The facts that a limited group of photoreceptor-specific antisera labels iguanid CSF-contacting neurons and that immunoreactivity differs between species have raised doubts about these cells functioning as photoreceptors. Hirunagi et al. (1993), using both rod- and cone-specific antisera, failed to find opsin-like immunoreactivity in the brains of a variety of reptilian species, and they argued that the difference between their results and those of others was not due to methodological differences, because their antisera labeled retinal and pineal photoreceptors. However, techniques that label retinal and pineal photoreceptors may not necessarily label an opsin-like antigen in the basal brain. Encephalic opsin-IR CSF-contacting neurons of nonmammalian vertebrates may be primordial photoreceptors; thus, they may be significantly different biochemically from retinal/pineal photoreceptors. The proteins of phototransduction in visual photoreceptors may have only limited homology with those of circadian/photoperiodic photoreceptors. In addition, the antigenic microenvironment may be different in different types of photoreceptors (see Vigh et al., 1982).

The morphology of opsin-IR CSF-contacting neurons is clearly distinct from retinal rods and cones, but it is similar to vertebrate pineal photoreceptors. At the concentration used in this study, the anticone opsin CERN-874 labels entire pinealocytes and CSF-contacting neurons, including the soma and putative axon, but it labels only the outer and inner segments of retinal photoreceptors (although previous studies have shown that the degree of immunolabeling in photoreceptor perikarya depends on the antibody concentration and fixation conditions; Vigh et al., 1982; Foster et al., 1987). Because of the intense immunoreactivity of the intraventricular terminal, it is possible that this structure is the principal photoreceptive region of the cell. However, the lack of retinal photoreceptor-like membranous stacks (outer segment disks) also distinguishes opsin-IR CSF-contacting neurons from visual photoreceptors of the retina. On the other hand, vertebrate pinealocytes range from cells with only a rudimentary 9+0 cilium to cells with lamellar membrane stacks that are very similar to retinal cones.

The presence of numerous large electron-dense vesicles in opsin-IR CSF-contacting neurons and the higher electron density of these vesicles in opsin-immunostained material suggest a relationship to some invertebrate extraretinal photoreceptors that also lack disk-like membranous stacks. Opsin-containing electron-dense vesicles of similar appearance (Robles et al., 1986), called lipochondria or photic vesicles, are concentrated in photosensitive neurons of the abdominal ganglion and in the cerebral ganglion of the gastropod mollusk *Aplysia californica*. The best

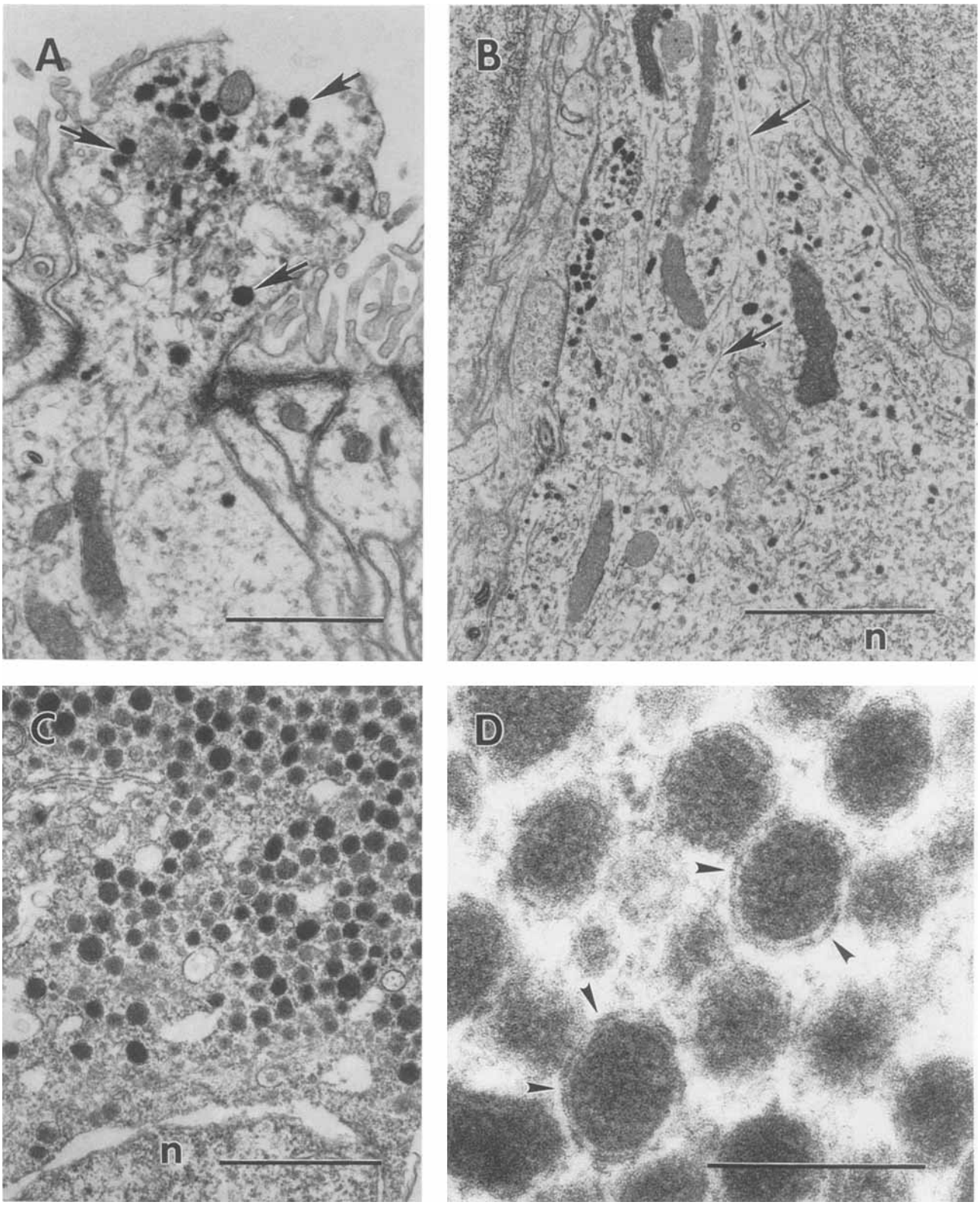

Fig. 11. Electron micrographs showing large (approximately 100 nm) electron-dense vesicles scattered throughout the soma, dendrites, and intraventricular terminals of opsin-immunostained CSF-contacting neurons. **A:** Electron-dense vesicles (arrows) in an *Iguana* opsin-IR neuron are highly concentrated in the intraventricular terminal (arrow). **B:** Vesicles do not appear associated with other subcellular structures such as microtubules (arrows; *Iguana*). **C:** Vesicles are highly concentrated throughout *Anolis* opsin-IR CSF-contacting neurons. The area shown is adjacent to the nucleus (n). **D:** High-power electron micrograph of an *Anolis* opsin-IR neuron showing that electron-dense vesicles are bounded by membrane (arrowheads) and exhibit a granular internal appearance. Scale bars = 1 μm in A,C, 2 μm in B, 0.2 μm in D.

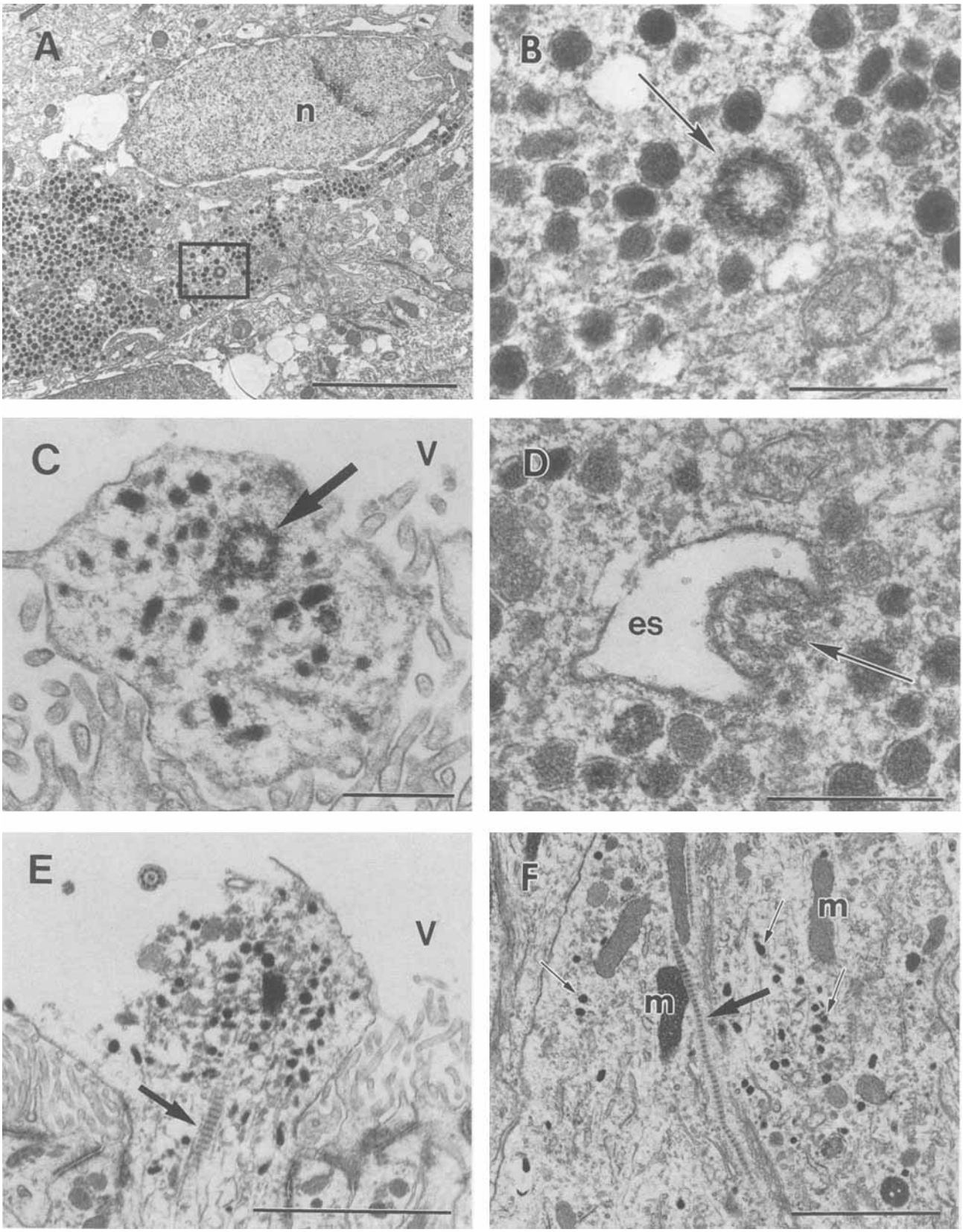

Fig. 12. Electron micrographs showing axonemes within opsin-IR CSF-contacting neurons. **A:** Cross section of an axoneme (rectangle) within the soma of an *Anolis* CSF-contacting neuron (n, nucleus). **B:** Higher magnification of the region enclosed in A showing axoneme in cross section (arrow). **C:** Axoneme cross section (arrow) within the intraventricular terminal of an *Iguana* CSF-contacting neuron (v, ventricle). **D:** Cross section of an axoneme (arrow) within an *Iguana* cell showing a "9+0" arrangement of doublet microtubules. The axoneme is subtended by a region of extracellular space (es). **E:** A ciliary rootlet (arrow) within the intraventricular terminal/dendrite of an *Iguana* opsin-IR CSF-contacting neuron (v, ventricle). **F:** A ciliary rootlet (arrow) coursing longitudinally through the putative dendrite of an *Iguana* CSF-contacting neuron (m, mitochondria; small arrows, electron-dense vesicles characteristic of opsin/VIP-IR CSF-contacting neurons). Scale bars = 3 μm in A, 0.5 μm in B–D, 2 μm in E,F.

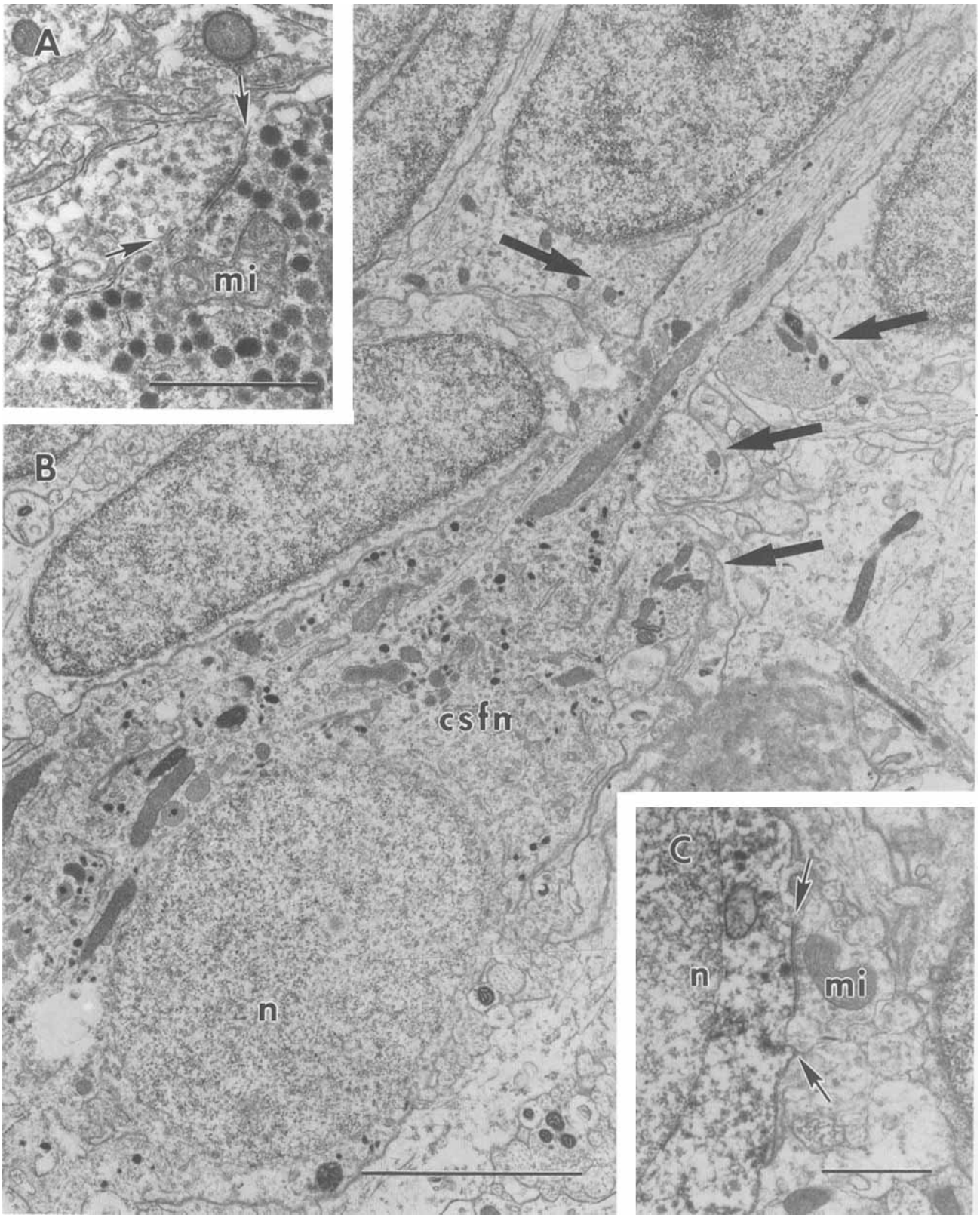

Fig. 13. Electron micrographs of synaptic contacts onto opsin- and VIP-IR CSF-contacting neurons of *Anolis* and *Iguana*. **A:** A synapse (arrows) onto an *Anolis carolinensis* opsin-IR CSF-contacting neuron whose mitochondrion (mi) is identified. **B:** Four synapses (arrows) occurring on the presumptive dendrite of a single opsin-IR CSF-contacting neuron (csfn) in *Iguana iguana*. **C:** A synapse onto the soma of a VIP-immunostained CSF-contacting neuron from *Iguana*. Note the presence of numerous small spherical electron-lucent vesicles, along with a smaller number of small electron-dense vesicles within the presynaptic terminals (n, nucleus). Scale bars = 1 μm in A,C, 3 μm in B.

studied of these neurons, the abdominal ganglion neuron R2, hyperpolarizes in response to light through an increase in plasmalemmal K^+ conductance (Andresen and Brown, 1982). The change in K^+ conductance is mediated by an increase in intracellular Ca^{2+} concentration (Brown et al., 1977), the probable source of which is the lipochondria. In response to illumination, lipochondria exhibit Ca^{2+} depletion (Brown et al., 1975) and ultrastructural changes (Brown et al., 1975; Henkart, 1975). Both light absorption and light-induced hyperpolarization of R2 peak at 490 nm, suggesting the involvement of a rhodopsin-like photopigment. *Aplysia* basal retinal neurons (BRNs) also contain large numbers of electron-dense vesicles. Many large (200–400 nm) electron-dense vesicles also occur in the photoreceptive *Bulla* BRNs (S.B. Khalsa, personal communication) as well as in opsin-IR neurons in the crayfish (*Cherax destructor*) cerebral ganglion (Sandeman et al., 1990).

VIP-like immunoreactivity has been described in CSF-contacting neurons of the nucleus accumbens/lateral septal region of several reptile species (Petko and Ihionvien, 1989; Hirunagi et al., 1993). Hirunagi et al. (1995) showed that the ultrastructure of VIP-IR cells of the duck lateral septal area is analogous to that of CSF-contacting neurons described by Vigh and Vigh-Teichmann (1988). These cells are also structurally analogous to the opsin- and VIP-IR cells that we describe here (Vigh and Vigh-Teichmann, 1988; Hirunagi et al., 1995). Silver et al. (1988) reported that VIP- and opsin-like immunoreactivity was colocalized in CSF-contacting neurons of several bird species but that only a subset of VIP-IR cells exhibit opsin-like immunoreactivity. Although we did not attempt to double label for opsin and VIP, our results suggest that most if not all of the VIP-IR CSF-contacting neurons of the basal lateral ventricles are also opsin-IR.

We propose that the opsin- and VIP-IR cells reported here may be photoreceptors mediating lights effects on circadian and reproductive rhythms. VIP is also implicated in both of these rhythms as well as in sleep. VIP-containing fibers contact gonadotropin-releasing hormone (GnRH)-positive neurons in the rat preoptic and anterior hypothalamic areas (van der Beek et al., 1993), and VIP affects the release of luteinizing hormone (Weick and Stobie, 1992). VIP stimulates serotonin-N-acetyltransferase and hydroxyindole-O-methyltransferase activities as well as melatonin production in the pineal gland (Moujir et al., 1992). Finally, infusion of VIP into the lateral ventricle causes significant changes in the sleep pattern of rats (Kruisbrink et al., 1987).

There is now good evidence that extraretinal photoreceptors mediating nonvisual responses to light exist in the basal brains of all four nonmammalian vertebrate classes (for review, see Foster et al., 1994). In birds and lizards, the eyes, pineal, and parietal are not required for circadian and photoperiodic responses to light. Whereas the eyes of mammals are required for reproductive photoperiodic responses and circadian entrainment by light, the photoreceptors mediating these effects may be either a small subclass of "conventional" retinal photoreceptors or a previously unrecognized class of retinal photoreceptive cells. The best evidence for this conclusion comes from studies on retinally degenerate mice, in which it has been shown that circadian responses to light remain unaffected at ages when mice have become completely blind visually (Foster et al., 1991; Provencio et al., 1994). It seems likely that, in all vertebrates, a unique class of irradiance-detecting photoreceptors mediates the effects of light on circadian and reproductive rhythms.

Why should two functional classes of photoreceptor, radiance and irradiance detectors, exist in vertebrates? Visual photoreceptors (radiance detectors) located within the eye form a precise spatial image of the environment by sampling large numbers of photons in a fraction of a second. Irradiance detection, however, requires that light be gathered from all directions and fall uniformly on an array of photoreceptors. This is precisely the effect achieved by having photoreceptors located within the brain. The tissues overlying extraretinal photoreceptors scatter light to such an extent that all directionality is lost. How, then, do mammals achieve irradiance detection using ocular (presumably retinal) photoreceptors? A recent tract-tracing study in sheep demonstrated that a group of retinal ganglion cells forms a nonretinotopic retinohypothalamic projection (Cooper et al., 1993). The authors suggest that the widespread arrangement of these cells within the retina increases sampling area, whereas their sparse numbers and their lack of retinotopic projection potentially preclude the detection of spatial contrast. In this way, mammals may have achieved efficient irradiance detection as well as increased sensitivity to the low levels of illumination present in the nocturnal niche in which they evolved (Foster and Menaker, 1994).

The results presented here form the first ultrastructural characterization of opsin-immunostained encephalic CSF-contacting neurons which are putative extraretinal, extrapineal photoreceptors involved in nonvisual responses to light. Our results show that cells predicted to be sensory neurons on the basis of morphology (see Vigh and Vigh-Teichmann, 1988) correspond to opsin- and VIP-IR cells predicted to mediate photoperiodism and circadian entrainment (Silver et al., 1988; Foster et al., 1993, 1994; Hirunagi et al., 1995). We show that these cells form a unique class of ependymal CSF-contacting neurons that share morphological and biochemical features with other vertebrate photoreceptors as well as with invertebrate extraretinal photoreceptors. To demonstrate that CSF-contacting neurons of the septal region of the brain are irradiance detectors mediating such responses to light, we must now show that they are directly photoreceptive (e.g., by electrical recording) and that their destruction abolishes responses of the circadian system to light.

ACKNOWLEDGMENTS

The authors thank Dr. W.J. DeGrip (University of Nijmegen, The Netherlands) for providing the antiopsin antisera and J.H. Spangenberg (Incstar, Inc., Stillwater, MN) for providing the anti-VIP antisera. This work was supported by NIH National Research Service Award institutional training grant DK07646 to M.S.G. and by National Institutes of Health grant HD13162 to M.M.

LITERATURE CITED

Andresen, M.C., and A.M. Brown (1982) Cellular basis of the photoresponse of an extraretinal photoreceptor. Experientia *38*:1001–1006.

Benoit, J. (1935) Le role des yeux dans l'action stimulante de la lumiere sur le developpement testiculaire chez le canard. C.R. Seances. Soc. Biol. Fil. *118*:669–671.

Benoit, J., and L. Ott (1944) External and internal factors in sexual activity. Effect of irradiation with different wavelengths on the mechanism of

photostimulation of the hypophysis and on testicular growth in the immature duck. Yale J. Biol. Med. *17:*27–46.

Brown, A.M., P.S. Baur Jr., and F.H. Tuley Jr. (1975) Phototransduction in *Aplysia* neurons: Primary event is calcium release from pigmented granules. Science *188:*157–160.

Brown, A.M., M.S. Brodwick, and D.C. Eaton (1977) Intracellular calcium and extraretinal photoreception in *Aplysia* giant neurons. J. Neurobiol. *8:*1–18.

Cooper, H.M., A. Tessonaud, A. Caldani, A. Locatelli, S. Richard, and M.C. Viguier-Martinez (1993) Morphology and distribution of retinal ganglion cells (RGC) projecting to the suprachiasmatic nucleus in the sheep. Soc. Neurosci. Abstr. *19:*1704.

Distel, H. (1976) Behavior and electrical brain stimulation in the green iguana, *Iguana iguana* L. I. Schematic brain atlas and stimulation device. Brain Behav. Evol. *13:*421–450.

Dixit, V.P., O.P. Sharma, and M. Agrawl (1977) The effects of light deprivations/blindings on testicular function of gerbil (*Meione horrianae*). Endocrinology *70:*13–18.

Foster, R.G., and M. Menaker (1993) Circadian Photoreception in Mammals and Other Vertebrates. In L. Wetterberg (ed): Light and Biological Rhythms in Man. Oxford: Pergamon. pp. 73–91.

Foster, R.G., H.G. Korf, and J.J. Schalken (1987) Immunocytochemical markers revealing retinal and pineal but not hypothalamic photoreceptor systems in the Japanese quail. Cell Tissue Res. *248:*161–167.

Foster, R.G., I. Provencio, D. Hudson, S. Fiske, W. De Grip, and M. Menaker (1991) Circadian photoreception in the retinally degenerate mouse (*rd/rd*). J. Comp. Physiol. A *169:*39–50.

Foster, R.G., J.M. Garcia-Fernandez, I. Provencio, and W.J. DeGrip (1993) Opsin localization and chromophore retinoids identified within the basal brain of the lizard *Anolis carolinensis*. J. Comp. Physiol. A *172:*33–45.

Foster, R.G., M.S. Grace, I. Provencio, W.J. DeGrip, and J.M. Garcia-Fernandez (1994) Identification of vertebrate deep brain photoreceptors. Neurosci. Biobehav. Rev. *18:*541–546.

Garcia-Fernandez, J.M., and R.G. Foster (1993) Immunocytochemical identification of photoreceptor proteins in hypothalamic CSF-contacting neurons of the larval lamprey (*Petromyzon marinus*). Cell Tissue Res. *275:*319–326.

Grace, M.S., V. Alones, M. Menaker, and R.G. Foster (1993) Correlated light and electron microscopy of opsin-immunoreactive neurons in the lizard basal brain. Soc. Neurosci. Abstr. *19:*1201.

Greenburg, N. (1982) A forebrain atlas and stereotaxic technique for the lizard *Anolis carolinensis*. J. Morphol. *174:*217–236.

Halberg, F., M.B. Visscher, and J.J. Bittner (1954) Relation of visual factors to eosinophil rhythms in mice. Am. J. Physiol. *179:*229–235.

Henkart, M. (1975) Light-induced changes in the structure of pigmented granules in *Aplysia* neurons. Science *188:*155–157.

Herbert, J., P.M. Stacey, and P.H. Thorpe (1978) Recurrent breeding seasons in pinealectomized or optic-nerve sectioned ferrets. J. Endocrinol. *78:*389–397.

Hirunagi, K., E. Rommel, A. Oksche, and H.-W. Korf (1993) Vasoactive intestinal peptide-immunoreactive cerebrospinal fluid-contacting neurons in the reptilian lateral septum/nucleus accumbens. Cell Tissue Res. *274:*79–90.

Hirunagi, K., E. Rommel, and H.-W. Korf (1995) Ultrastructure of cerebrospinal fluid-contacting neurons immunoreactive to vasoactive intestinal peptide and properties of the blood-brain barrier in the lateral septal organ of the duck. Cell Tissue Res. *279:*123–133.

Homma, K., and Y. Sakakibara (1971) Encephalic photoreceptors and their significance in photoperiodic control of sexual activity in Japanese quail. In M. Menaker (ed) Biochronometry. Washington D.C.: Natl. Acad. Sci., pp. 333–341.

Homma, K., Y. Sakakibara, and M. Ohta (1977) Potential sites and action spectra for encephalic photoreception in the Japanese quail. In B.K. Follett (ed): First International Symposium on Avian Endocrinology. University College of North Wales, pp. 25–26.

Kruisbrink, J., M. Mirmiran, T.P. Van der Woude, and G.J. Boer (1987) Effects of enhanced cerebrospinal fluid levels of vasopressin, vasopressin antagonist, or vasoactive intestinal polypeptide on circadian sleep-wake rhythm in the rat. Brain Res. *419:*76–86.

McMillan, J.P., H.C. Keatts, and M. Menaker (1975a) On the role of eyes and brain photoreceptors in the sparrow: Entrainment to light cycles. J. Comp. Physiol. *102:*251–256.

McMillan, J.P., H.A. Underwood, J.A. Elliott, M.H. Stetson, and M. Menaker (1975b) Extraretinal light perception in the sparrow. IV. Further evidence that the eyes do not participate in photoperiodic photoreception. J. Comp. Physiol. *97:*205–213.

Menaker, M., and H. Keatts (1968) Extraretinal light perception in the sparrow II: Photoperiodic stimulation of testis growth. Proc. Natl. Acad. Sci. USA *60:*146–151.

Menaker, M., and S. Wisner (1983) Temperature-compensated circadian clock in the pineal of *Anolis*. Proc. Natl. Acad. Sci. USA *80:*6119–6121.

Menaker, M., R. Roberts, J. Elliott, and H. Underwood (1970) Extraretinal light perception in the sparrow III: The eyes do not participate in photoperiodic photoreception. Proc. Natl. Acad. Sci. USA *67:*320–325.

Moujir, F., B.A. Richardson, K. Yaga, and R.J. Reiter (1992) Vasoactive intestinal polypeptide stimulates N-acetyltransferase and hydroxyindole-O-methyltransferase activities and melatonin production in cultured rat but not in Syrian hamster pineal glands. J. Pineal Res. *12:*35–42.

Nelson, R.J., and I. Zucker (1981) Absence of extraocular photoreception in diurnal and nocturnal rodents exposed to direct sunlight. Comp. Biochem. Physiol. *69A:*145–148.

Oliver, J., and J.D. Bayle (1976) The involvement of the preoptic-suprachiasmatic region in the photosexual reflex in quail: Effects of selective lesions and photic stimulation. J. Physiol. (Paris) *72:*627–637.

Oliver, J., C. Bouille, S. Herbute, and J.D. Bayle (1977a) Horseradish peroxidase study of intact or deafferented infundibular complex in *Coturnix* quail. Neuroscience *2:*989–996.

Oliver, J., S. Herbute, and J.D. Bayle (1977b) Testicular response to photostimulation by radioluminous implants in the deafferented hypothalamus of quail. J. Physiol. (Paris) *73:*685–691.

Oliver, J., M. Jallageas, and J.D. Bayle (1979) Plasma testosterone and LH levels in male quail bearing hypothalamic lesions or radioluminous implants. Neuroendocrinology *28:*114–122.

Oliver, J., M. Jallageas, B. Sicard, and J.D. Bayle (1980) Testicular responses to local stimulation of the lobus paraolfactorius in quail. J. Physiol. (Paris) *76:*611–616.

Petko, M., and M. Ihionvien (1989) Distribution of substance P, vasoactive intestinal polypeptide and serotonin immunoreactive structures in the central nervous system of the lizard, *Lacerta agilis*. J. Hirnforsch. *30:*415–423.

Provencio, I., E.R. Loew, and R.G. Foster (1992) Vitamin A_2-based visual pigments in fully terrestrial vertebrates. Vision Res. *32:*2201–2208.

Provencio, I., S. Wong, A.B. Lederman, S.M. Argamaso, and R.G. Foster (1994) Visual and circadian responses to light in aged retinally degenerate (*rd*) mice. Vision Res. *34:*1799–1806.

Robles, L.J., J.W. Breneman, E.O. Anderson, V.A. Nottoli, and L.L. Kegler (1986) Immunocytochemical localization of a rhodopsin-like protein in the lipochondria in photosensitive neurons of *Aplysia californica*. Cell Tissue Res. *244:*115–120.

Sandeman, D.C., R.E. Sandeman, and H.G. de Couet (1990) Extraretinal photoreceptors in the brain of the crayfish *Cherax destructor*. J. Neurobiol. *21:*619–629.

Sicard, B., J. Oliver, and J.D. Bayle (1983) Gonadotropic and photosensitive abilities of the lobus paraolfactorius: Electrophysiological study in quail. Neuroendocrinology *36:*81–87.

Silver, R., P. Witkovsky, P. Horvath, V. Alones, C.J. Barnstable, and M.N. Lehman (1988) Coexpression of opsin- and VIP-like-immunoreactivity in CSF-contacting neurons of the avian brain. Cell Tissue Res. *253:*189–198.

Takahashi, J.S., N. Murakami, S.S. Nikaido, B.L. Pratt, and L.M. Robertson (1989) The avian pineal, a vertebrate model system of the circadian oscillator: Cellular regulation of circadian rhythms by light, second messengers, and macromolecular synthesis. Rec. Progr. Horm. Res. *45:*279–352.

Underwood, H., and M. Menaker (1970) Extraretinal light perception: Entrainment of the biological clock controlling lizard locomotor activity. Science *170:*190–193.

Underwood, H., and M. Menaker (1976) Extraretinal photoreception in lizards. Photochem. Photobiol. *23:*227–243.

van der Beek, E., V.M. Wiegant, H.A. Van der Donk, R. Van den Hurk, and R.M. Buijs (1993) Lesions of the suprachiasmatic nucleus indicate the presence of a direct vasoactive intestinal polypeptide-containing projection to gonadotropin-releasing hormone neurons in the female rat. J. Neuroendocrinol. *5:*137–144.

Vigh, B., and I. Vigh-Teichmann (1988) Comparative neurohistology and immunocytochemistry of the pineal complex with special reference to CSF-contacting neuronal structures. Pineal Res. Rev. *6:*1–65.

Vigh, B., I. Vigh-Teichmann, P. Röhlich, and B. Aros (1982) Immunoreactive opsin in the pineal organ of reptiles and birds. Z. Mikrosk. Anat. Forsch. *96:*113–129.

Vigh, B., I. Vigh-Teichmann, P. Röhlich, and A. Oksche (1983) Cerebrospinal fluid-contacting neurons, sensory pinealocytes and Landolt's clubs of the retina as revealed by means of electro-microscopic immunoreaction against opsin. Cell Tissue Res. *233:*539–548.

Vigh-Teichmann, I., P. Röhlich, B. Vigh, and B. Aros (1980) Comparison of the pineal complex, retina and cerebrospinal fluid-contacting neurons by immunocytochemical antirhodopsin reaction. Z. Mikrosk. Anat. Forsch. *94:*623–640.

Vigh-Teichmann, I., B. Vigh, H.-W. Korf, and A. Oksche (1983) CSF-contacting and other somatostatin-immunoreactive neurons in the brains of *Anguilla anguilla*, *Phoxinus phoxinus*, and *Salmo gairdneri* (Teleostei). Cell Tissue Res. *233:*319–334.

Weick, R.F., and K.M. Stobie (1992) Vasoactive intestinal polypeptide inhibits the steroid-induced LH surge in the ovariectomized rat. J. Endocrinol. *133:*433–437.

Yokoyama, K., A. Oksche, T.R. Darden, and D.S. Farner (1978) The sites of encephalic photoreception in the photoperiodic induction of growth of the testes in the white crowned sparrow, *Zonotrichia leucophrys gambelii*. Cell Tissue Res. *189:*441–467.